JOURNAL OF APPLIED ELECTROCEMISTRY 13 (1983) 541–548

Electrochemical aspects of the codeposition of gold and copper with inert particles

C. BUELENS, J. P. CELIS, J. R. ROOS

Department Metaalkunde, K. U. Leuven, De Croylaan 2, Heverlee, Belgium

Received 4 October 1982

In the present paper, data on the codeposition of fine Al_2O_3 particles with copper from an acidified copper sulphate bath and on the codeposition of Au–Al_2O_3 from a gold cyanide bath are compared. Based on these results, it is shown that the mechanism of codeposition of inert particles is similar in both systems. The reduction of ions adsorbed on alumina particles is the rate-determining step. The rate of codeposition is further dependent on the mass transport to the electrode and on the applied voltage.

Based on the information gained from these experiments on the electrolytic codeposition of inert particles with a metal, the electrolytic deposition process of the pure metal and the incorporation of foreign ionic species in such an electrolytic deposit are discussed.

1. Introduction

In the present paper the process of electrolytic codeposition of inert particles with metals is investigated. Data on the codeposition of Cu–Al_2O_3 from an acidified copper sulphate bath and on the codeposition of Au–Al_2O_3 from an additive free gold cyanide bath are compared. Based on these results more insight into the process and mechanism of electrolytic codeposition of inert particles is gained. The usefulness of this knowledge in acquiring a better understanding of the electrolytic deposition process of the metal itself is discussed.

1.1. *Electrolytic codeposition of inert particles with metals*

Electrolytic codeposition of inert particles with metals has been discussed since 1969 as a production method for composite coatings. The electrolytic preparation of composites is based on the ability to embed in a metal matrix during electrolysis, inert particles suspended in the plating bath. This phenomenon has been known since conventional electrolysis was first developed. The formation of rough deposits was attributed to the presence of 'impurities' in the plating baths. To avoid such rough deposits impurities have to be removed e.g., by bath purification. The possibility to codeposit foreign particles is used but in a controlled way to obtain composite coatings by electrolysis. A scanning electron micrograph of an as-plated copper–silicon carbide composite made from an acidified copper sulphate bath is shown in Fig. 1. The inert particles have to be kept in suspension by either mechanical stirring or by using appropriate surfactants. In the latter case, special care has to be taken to avoid flotation of the particles.

Electrolysis conditions to obtain a composite with well-defined characteristics cannot yet be described. Actual insight into the mechanism of codeposition is not sufficient to fully predict the influence of electrolysis conditions on codeposition. Three possible mechanisms of codeposition are generally accepted, namely: (1) particles can be transferred to the cathode by an electrophoretic action to be keyed into the matrix during the electrolytic deposition. (2) particles can be brought up against the cathode by bath agitation where they are embedded into the electrolytically deposited matrix (mechanical entrapment). (3) particles can be adsorbed onto the cathode due to van der Waals' attractive forces holding particles at the cathode.

Recent theoretical and experimental work [1–6] clarifies the relative importance of these three possible mechanisms. Electrolytic codeposition

0021-891X/83 $03.00 + .12. © 1983 Chapman and Hall Ltd.

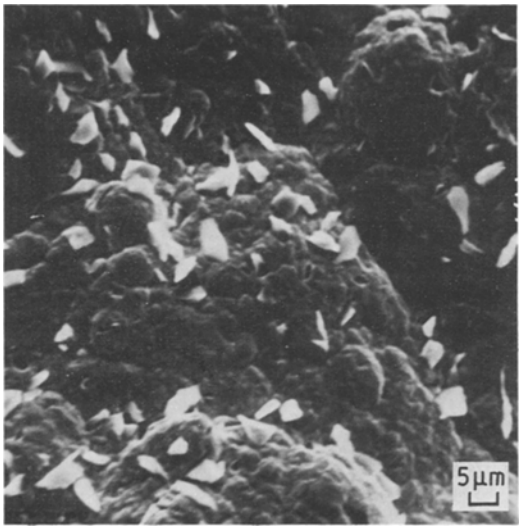

Fig. 1. SEM Micrograph of a Cu–SiC composite coating. Plating bath, 30 g dm^{-3} Cu^{2+} + 120 g dm^{-3} H_2SO_4 + 50 g dm^{-3} SiC (± 3 µg); room temperature (20° C), current density, 5 A dm^{-2}.

seems to be dependent on two types of adsorption processes (Fig. 2) namely adsorption of ions on the inert particles and adsorption of particles on the cathode surface. Concerning the adsorption of particles on the cathode, the mathematical model of Guglielmi [1] has already been shown to be valid for various systems [1–3]. The effectiveness of the adsorption of particles on the cathode, however, is dependent on the preceeding process of adsorption of ionic species onto the particles suspended in the plating solution [4–6].

1.2. *Electrolytic deposition processes of Cu and Au*

The copper deposition reaction can be regarded as being composed of two steps, each of which involves the transfer of an electron:

$$Cu^{2+} + e^- \rightleftharpoons Cu^+ \quad \text{(slow)} \qquad (1)$$

$$Cu^+ + e^- \rightleftharpoons Cu \quad \text{(fast)} \qquad (2)$$

$$Cu^{2+} + 2\,e^- \rightleftharpoons Cu \qquad (3)$$

These electrode reactions have already been studied extensively for solutions of copper sulphate and sulphuric acid [7, 8].

The mechanism of reduction of gold complexes in cyanide solution, is not fully understood and still needs further investigation. According to

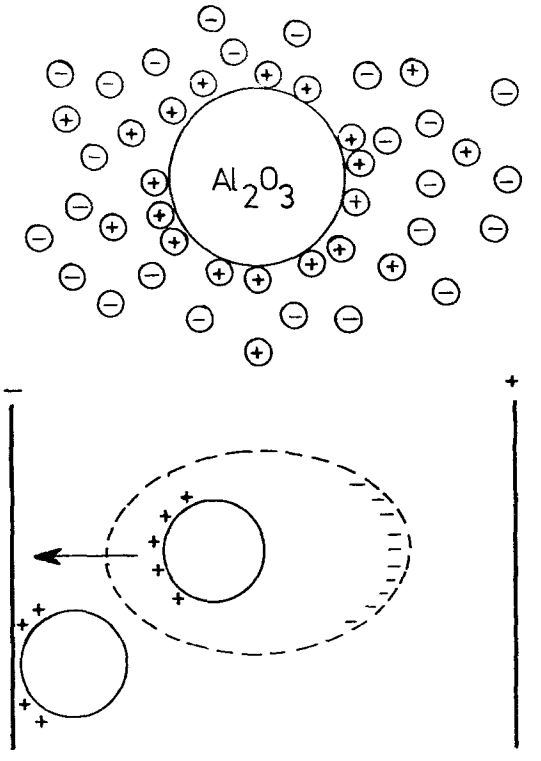

Fig. 2. Schematic representation of important adsorption phenomena in codeposition. On inert Al_2O_3 particles and on a cathode surface.

Ibl and Angerer [9] the potassium gold cyanide dissociates into a $Au(CN)_2^-$ complex. The reduction of the latter complex involves two steps:

$$Au(CN)_2^- \rightarrow Au(CN) + CN^- \qquad (4)$$

This homogeneous pre-reaction takes place in the diffusion layer. The reaction product Au(CN) can either be adsorbed or may form an insoluble film at the electrode. The second step is a reduction of this Au(CN).

$$Au(CN) + e^- \rightarrow Au + CN^-. \qquad (5)$$

In acid solutions this CN^- can react with protons:

$$H_3O^+ + CN^- \rightarrow H_2O + HCN. \qquad (6)$$

This HCN can escape in the atmosphere or dissolve into the solution creating different polymers, as $(HCN)_x$.

2. Experimental procedure

For the electrodeposition tests flat vertical electrodes and rotating disc electrode (RDE)

assemblies were used in combination with an electrochemical measurement apparatus. When flat vertical electrodes were used, the alumina particles were kept in suspension by mechanical stirring using a vibrating perforated bottom plate. As rotating disc electrodes several electrodes with different shaped insulating sheaths have been used: Shaped electrodes of the Riddiford type, made from a polyester resin (outer diameter, 80 mm) containing platinum (3 mm) or stainless steel (60 mm) discs as active electrode surface (see Fig. 3a). Cylindrical PTFE electrodes (outer diameter, 54 mm) with an interchangeable bottom made of profiled thin brass sheet (30 mm) as active electrode surface (Fig. 3b and c).

All electrodes used in the present study are disc electrodes for which the fluid flow to the active area located at the bottom of the electrode has to be taken into account.

The d.c.-motor used (type Mavilor 80W) allows a reproducible constant rotation speed between 10 and 6000 rpm. No extra mechanical stirring was required to keep the alumina particles in suspension. This set-up is especially attractive for the study of electrolytic codeposition since it allows control of the fluid flow towards the working electrode. The rotating disc electrode allows the creation of reproducible conditions with known constant hydrodynamic mass transport. The flow in the vicinity of the rotating disc is fixed and was calculated exactly by Levich [12]. On the disc a thin layer of fluid rotates with the disc at the same rotation speed. This layer is called the hydrodynamic boundary layer. Thus tangential velocity of the fluid decreases perpendicular from the disc. The radial velocity component is maximal when the thickness of the hydrodynamic boundary layer is reached. The fluid flows to the side of the disc by centrifugal force. An axial flow towards the disc instantly compensates for this loss of fluid. The whole disc acts as a pump, that brings the inert particles in suspension, sucks the fluid, rotates it and then moves it to the side. One can easily establish laminar or turbulent flow by increasing the rotation speed. If the working electrode is polarized, the convective diffusion controls the transport of species from the bulk to the electrochemical double layer and that layer is fixed with the RDE. By controlling the potential of the electrode, charge transfer or concentration overvoltage conditions can be created and evaluated under known mass transport conditions.

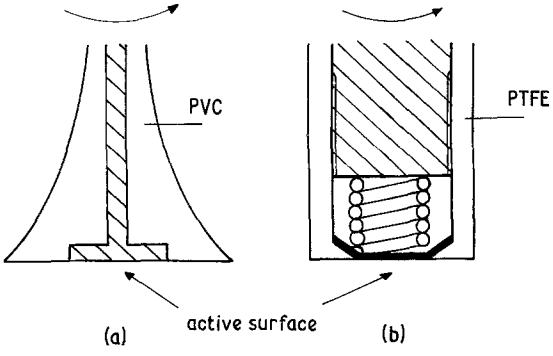

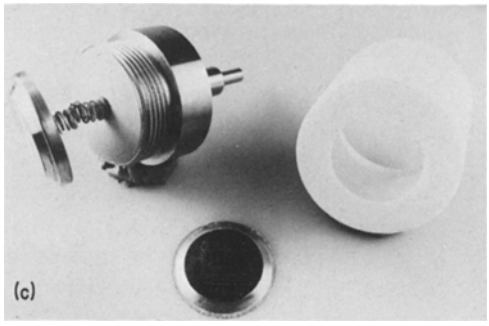

Fig. 3. Cylindrical PTFE-electrode with interchangeable bottom.

Electrochemical transients such as linear polarisation measurements and small-amplitude cyclic voltammetry were performed on the RDE to study the process taking place at the electrode surface during codeposition. A three-electrode cell with a platinized titanium grid counter electrode and a saturated calomel reference electrode, was connected to a PAR model 173/376 potentiostat and a PAR model 175 function generator. All chemicals used were pa grade. Experimental conditions are listed in Table 1. The determination of the alumina content has been done for copper by a wet chemical analysis technique and for gold by X-ray fluorescence spectrometry.

All deposits were made in the galvanostatic mode; polarization curves and cyclic voltammetry experiments were performed under potentiostatic control.

3. Results and discussion

The effect of the rotation speed of the electrode on the amount of codeposited γ-alumina particles is

Table 1. Bath characteristics used in this study

Process	*Plating Bath*	*Temperature* °C	pH
Copper plating	Acidified copper sulphate Cu 30 g dm^{-3} (as $CuSO_4 \cdot 5H_2O$) H_2SO_4 120 g dm^{-3}	Room temperature (20)	0.03
Gold plating	Additive free Au 10 g dm^{-3} (as $KAu(CN)_2$) KH_2PO_4 100 g dm^{-3}	40	4

shown in Figs. 4 and 5 for the systems Cu–Al_2O_3 and Au–Al_2O_3 respectively. These experiments on copper plating were done using a shaped disc electrode (Fig. 3a), whereas a cylindrical disc electrode (Fig. 3b) was used for the gold plating experiments. A comparison between Figs. 4 and 5 shows a shift in rotation speed at which laminar, transition and turbulent flow patterns are found. This is due to the use of disc electrodes with different shape and size. From the formula for the Reynolds number given below:

$$Re = \frac{\omega R^2}{\nu}$$

where R is the radius of disc electrode, ω the rotation speed and ν is the kinematic viscosity of the fluid, it can be deduced that, for disc electrodes of different size, the same Re number will correspond to different rotation speeds. The different shape, furthermore, is responsible for the experimentally determined shift of rotation speed at the transition from laminar to turbulent flow regime. Zones of laminar, transition and turbulent hydrodynamic flow for these rather large electrodes have been determined based on motor couple – rotation speed diagrams [13]. On such graphs three straight lines with different slopes are noticed, each of which can be related to one of the hydrodynamic flow regions. The intersection of two lines corresponds with the transition between two zones. In the case of shaped disc electrode the values of the Re numbers at the transitions in flow regimes in a copper sulphate solution are:

$$Re_{\text{lam-trans}} = 3.7 \times 10^4$$

$$Re_{\text{trans-turb}} = 1 \times 10^5$$

From Fig. 4 it can be deduced that under laminar flow conditions a constant amount of Al_2O_3 particles is embedded. At the start of the transition zone a marked decrease in embedded alumina is noticed. At increasing rotation speed an important increase of embedded alumina is determined until the turbulent zone is reached, where an abrupt decrease of the amount of embedded alumina occurs. The increased amount

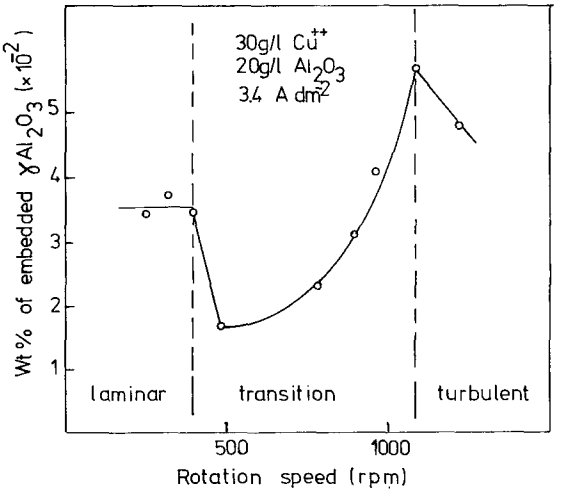

Fig. 4. Wt % of embedded Al_2O_3 in copper against rotation speed of rotating Riddiford type electrode.

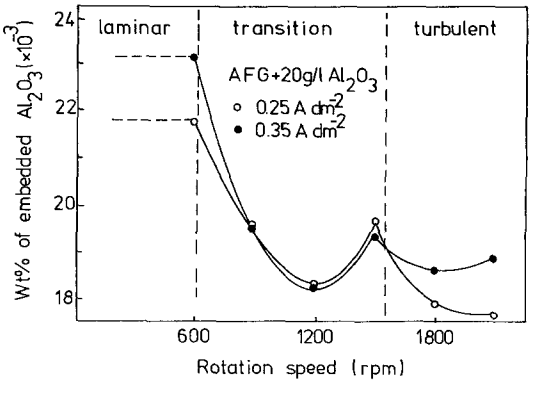

Fig. 5. Wt % of embedded Al_2O_3 in gold versus rotation speed of rotating cylindrical electrode.

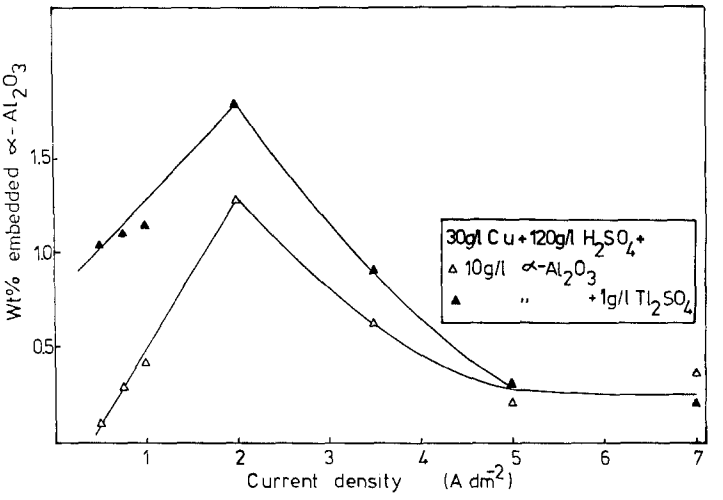

Fig. 6. Wt % of embedded alumina against current density for deposits obtained from an acidified copper sulphate solution on a flat vertical cathode [14].

of codeposited alumina in the transition zone has been shown to be due to the formation of Al_2O_3-agglomerates in the solution and the subsequent codeposition of such agglomerates [13]. For the Au–Al_2O_3 system (Fig. 5) a similar pattern has been determined.

The effect of the current density on the amount of codeposited inert particles is shown in Figs. 6 and 7 for the copper–alumina and the gold–alumina systems respectively. The copper–alumina deposits were obtained on a flat vertical electrode, the gold–alumina deposits on a rotating cylindrical electrode. In Fig. 6 the increased codeposition of α-Al_2O_3 with copper due to the addition of the monovalent cation Tl^+ is shown [2, 14]. Similar results were obtained for the codeposition of γ-alumina with copper, but at lower wt % of embedded particles. In Fig. 7 the effect of rotation speed of the electrode on the position and height of the maxima of codeposited Al_2O_3 particles with gold is shown. At increasing rotation speed, a shift of the maxima towards higher current densities seems to be the rule.

From Figs. 6 and 7 it can be seen that, even under totally different electrolysis conditions, but still in the range where flat deposits are obtained, the weight percentage of embedded alumina particles against current density always shows one (Cu–Al_2O_3 system) or more (Au–Al_2O_3 system) maxima. Recently White and Foster [6] confirmed this relationship for the deposition of alumina from copper sulphate solutions.

From a technical viewpoint, it is important to notice that, according to literature, the carbon and cobalt contents of gold deposits also show a maximum (around 0.5 wt %) in the low current density range (1 to 4 A dm^{-2} for *Re* numbers of 2900 to 13400 respectively) [9]. In as much as the results of carbon or cobalt incorporation and the codeposition of suspended fine particles are comparable (different *Re*, different systems) it may be assumed that both processes occur by a similar mechanism, namely the entrapment by a subsequent reduction step of some solid species adsorbed on the cathode surface. Our theory is in agreement with Eisenmann's conclusion [15] that for a cobalt containing gold cyanide solution the incorporated compound is a $KCo[Au(CN)_2]_3$ precipitate. For cobalt free solutions the incorporation of polymers such as $(HCN)_4$ has already been mentioned [16].

Polarization curves have been recorded in

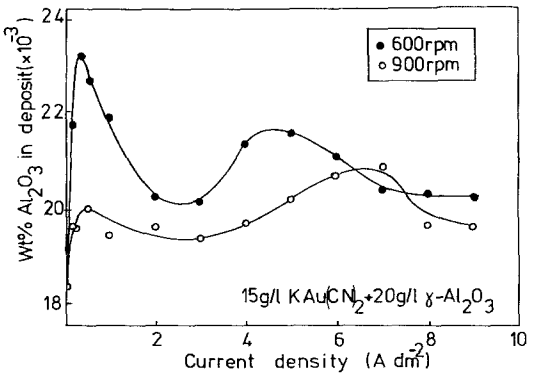

Fig. 7 Wt % of embedded γ-alumina against current density at different rotation speeds of a rotating cyclindrical electrode.

copper sulphate and gold cyanide solutions in absence and in presence of alumina particles. In Fig. 8 the polarization measurements obtained in a copper sulphate bath on a flat vertical cathode are plotted. Similar plots for the gold cyanide solution on a rotating cylindrical disc electrode are given in Fig. 9. From these polarization curves recorded in absence and in the presence of alumina particles it seems that, although the general shape of the polarization curve is unaffected by the addition of alumina particles, in the presence of alumina particles the curve is shifted towards lower overpotentials for an identical current density.

A comparison of polarization curves and wt% of embedded Al_2O_3 versus current density curves was done in a previous extensive study of $Cu-Al_2O_3$ electrolytic codeposition [14]. In that study it was shown that at current densities for which a considerable increase of the amount of embedded alumina particles at increasing current density appears, the reduction of copper ions is under charge-transfer overvoltage control. Once the reduction of copper ions is under concentration overvoltage control ($> 2\ A\,dm^{-2}$ in the case shown in Fig. 8) the amount of codeposited alumina decreases gradually at increasing current densities. The dependency of codeposition on charge-transfer overvoltage indicates that the rate of codeposition is determined by the formation of a real contact between the alumina particles and the cathode. As shown by different researchers [4, 5, 17], on immersion of alumina particles in the plating solution, adsorption of cations as H^+ and Cu^{2+} onto the particles occurs. It seems thus that the real contact results from the reduction of

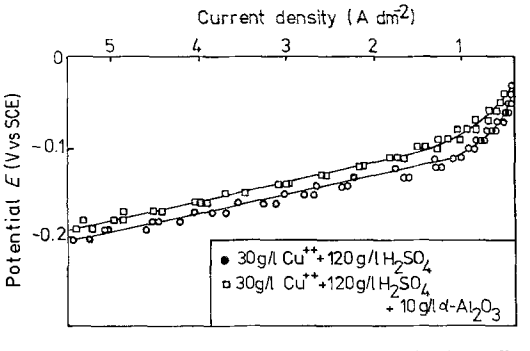

Fig. 8. Polarization curves of copper recorded using a flat vertical electrode in a mechanically stirred copper sulphate solution.

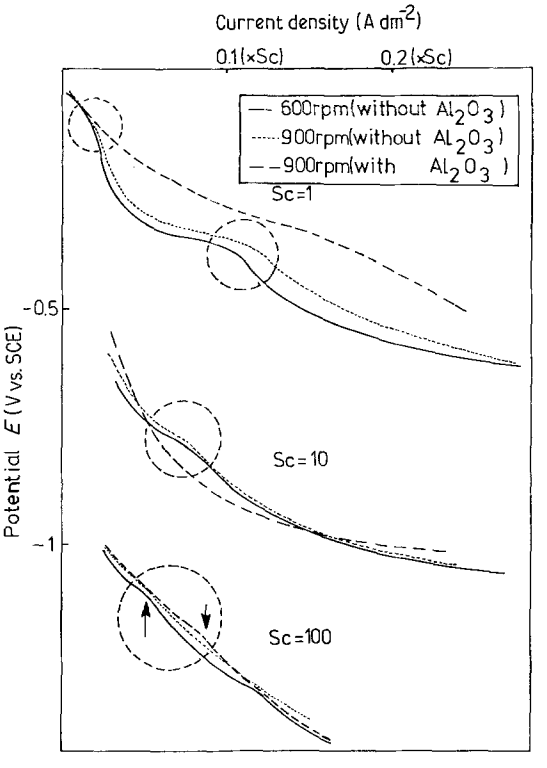

Fig. 9. Polarization curves of gold recorded in a 15 g dm^{-3} $KAu(CN)_2$ + 100 g dm^{-3} KH_2PO_4 at different rotation speeds of the rotating cylindrical electrode.

the copper ions adsorbed on the alumina particles. This reduction of adsorbed ions is thus the rate-determining step. Thallium ions which promote codeposition, seem to act as a catalyst for the copper reduction reaction. Adsorbed cations on alumina play a two-fold role: they increase the attraction of particles to the cathode surface, and the reduction of adsorbed species creates a real contact between cathode and particles.

Concerning the codeposition of alumina from gold cyanide solutions, it can be postulated that on immersion of alumina particles an adsorption of some gold cyanide complexes occurs. The reduction from such solutions is already explained above. The polarization curves for pure gold plotted in Fig. 9 show four kinks namely at potentials of about -0.1, -0.4, -0.75 and -1.15 V versus SCE. These kinks seem to indicate a transition from a charge transfer controlled process to a process dominated by concentration overpotential leading to a limiting current density. A detailed description of these different processes

Table 2. Type of alumina powder used in this study

	Alumina powder	
	α	γ
Product	Linde A 810–783	Linde B 810–779
Mean size	0.3 μm	0.05 μm
Structure	hexagonal (α) type	Spinel cubic (γ) type

was not found in the literature. However for a 15 g dm^{-3} potassium gold cyanide bath (pH 3.5) containing citric acid and cobalt acetate. Ibl and Angerer [9] reported that the limiting current plateaus observed below 0.2 A dm^{-2} are probably due to the synergetic effect of the transport controlled reduction of dissolved oxygen. Further studies have to be done to identify the species involved in the third and fourth kink.

Combination of Fig. 7 and Fig. 9 gives a plot of wt % of embedded alumina versus electrode overpotential. From such a graph (Fig. 10) it can be concluded that the two codeposition maxima occur at potentials of about -0.75 V and -1.15 V versus SCE. These potentials are unaffected by the rotation speed of the cylindrical disc electrode, only the height of the maxima being dependant on rotation speed. It seems now that these maxima occur at potentials at which the third and fourth kink in the polarization curve were found (cf. Fig. 9). From the analogy with the charge transfer overvoltage dependency in the Cu–Al_2O_3 system, a possible explanation for these maxima can thus be a reduction under charge transfer overvoltage control of different gold species present in the solution and adsorbed on the alumina particles. The large dependency of the height of the first maximum on rotation speed can perhaps be explained by a riding effect of particles on the growing surface as proposed by White and Foster [6]. The fact that the second maximum is not so strongly dependent on the rotation speed, confirms the hypothesis that at this higher overpotential another gold species is reacting which reduction causes a stronger bonding of particles to the cathode surface.

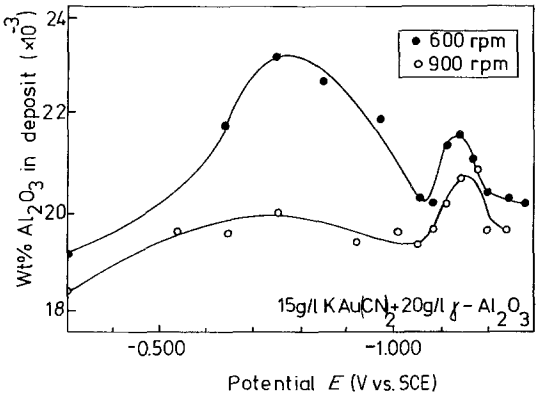

Fig. 10. Wt % of embedded γ-alumina against electrode potential of a rotating cylindrical electrode calculated from Figs 6 and 8.

The scientific importance of the experimental technique used in the present study, i.e., the combined use of rotating electrodes and electrochemical control by potentiostat, can be found in the broadening of the insight into the mechanism of electrolytic codeposition of inert particles. Our experimental results support the importance of two adsorption processes namely the adsorption of species on particles and the adsorption of particles onto the cathode. Codeposition occurs once adsorbed species are electrochemically reduced at the cathode surface. Based on the analogy between the incorporation of Cu and Co and the codeposition of fine inert particles, as already explained above, the knowledge about the latter system can be used for understanding the first, not so well known system.

4. Conclusions

From a comparison of the electrolytic codeposition of alumina with copper from an acidified copper sulphate solution and with gold from an additive free gold cyanide solution, it was shown that the mechanism of codeposition is similar for both systems. The reduction of ions adsorbed on alumina particles is the rate determining step. The rate of codeposition is further dependent on the mass transport to the electrode, as shown by the dependency of codeposition on the hydrodynamic flow conditions existing along the disc electrode,

and on the applied overvoltage. A large increase in codeposition is observed each time the reduction of the main metal species is under charge-transfer overvoltage control.

Based on the relationship between wt% of embedded particles and overpotential, it was possible to demonstrate that in an additive free gold cyanide solution, different gold species are reduced at potentials of -0.75 and -1.15 V versus SCE. The analogy between the incorporation of fine suspended solid particles and the incorporation of carbon and cobalt from gold cyanide solution allows us to assume a similar mechanism of incorporation of foreign species as C and Co in gold deposits. The presence of fine suspended solid C and Co compounds in the plating solution is presumed and these solid compounds might be incorporated after being adsorbed onto the cathode only in a well defined overpotential range.

References

[1] N. Guglielmi, *J. Electrochem. Soc.* **119** (1972) 1009.
[2] J. P. Celis and J. R. Roos, *ibid.* **124** (1977) 1502.
[3] R. Narayan and B. Narayana, *Rev. Coatings Corros.* **4** (1981) 113.
[4] J. R. Roos, J. P. Celis and J. A. Helsen, *Trans. Inst. Met. Fin.* **55** (1977) 113.
[5] T. W. Tomaszewski, *ibid.* **54** (1976) 45.
[6] C. White and J. Foster, *ibid.* **59** (1981) 8.
[7] O. R. Brown and H. R. Thirsk, *Electrochim. Acta* **10** (1965) 383.
[8] E. Mattson and J. O. M. Bockris, *Trans. Faraday Soc.* **55** (1959) 1586.
[9] N. Ibl and M. Angerer, *J. Appl. Electrochem* **9** (1979) 219.
[10] F. B. Koch, Y. Okinaka, C. Wolowodiuk and D. R. Blessington, *Plat. Surf. Fin.* (1980) 50.
[11] *Idem, ibid.* (1980) 43.
[12] V. G. Levich, 'Physicochemical Hydrodynamics', Prentice Hall, Englewood Cliffs, New Jersey (1962).
[13] J. R. Roos, J. P. Celis, H. Kelchtermans, M. Van Camp and C. Buelens, Proceedings of 10th World Congress on Metal Finishing, (edited by S. Hawyama) The Metal Finishing Society of Japan, Kyoto, (1980) p. 203.
[14] J. P. Celis, Ph.D. thesis, K. U. Leuven, Dept. Metaalkunde (1976).
[15] E. T. Eisenmann, *J. Electrochem. Soc.* **124** (1977) 1957.
[16] H. G. Silver, *ibid.* **116** (1969) 591.
[17] A. M. J. Kariapper, J. Foster, *Trans, Inst. Met. Fin.* **52** (1974) 87.